On carbide dissolution in an as-cast ASTM F-75 alloy

M. Caudillo,[1] M. Herrera–Trejo,[1] M. R. Castro,[1] E. Ramírez,[1] C. R. González,[2] J. I. Juárez[2]
[1]*CINVESTAV IPN-Unidad Saltillo, Apartado Postal 663, C.P. 25000 Saltillo, Coah., México*
[2]*Dpto. Ingeniería Metalúrgica, Fac. De Química, UNAM, Circuito Exterior S/N, Edif. D, Cd Universitaria, 04510, México, D.F., México*

Received 8 February 2001; accepted 6 July 2001

Abstract: The solution treatment of an as-cast ASTM F-75 alloy was investigated. Microstructural evolution was followed during thermal processing, in particular with regard to the content and type of carbides formed. To evidence any probable carbide transformations occurring during the heating stage, as well as to clarify their effect on the carbide dissolution kinetics, three heating rates were studied. Image analysis and scanning electron microscopy techniques were used for microstructural characterization. For the identification of precipitates, these were electrolytically extracted from the matrix and then analyzed by X-ray diffraction. It was found that the precipitates in the as-cast alloy were constituted by both a $M_{23}C_6$ carbide and a σ intermetallic phase. The $M_{23}C_6$ carbide was the only phase identified in solution-treated specimens, regardless of the heating rate employed, which indicated that this carbide dissolved directly into the matrix without being transformed first into an M_6C carbide, as reported in the literature. It was found that the kinetics of dissolution for the $M_{23}C_6$ carbide decreased progressively during the solution treatment, and that it was sensitive to the heating rate, decreasing whenever the latter was decreased. Because the $M_{23}C_6$ carbide was not observed to suffer a phase transformation prior to its dissolution into the matrix, the effect of the heating rate was associated to the morphological change occurred as the specimens were heated. The occurrence of the observed phases was analyzed with the aid of phase diagrams computed for the system Co–Cr–Mo–C. © 2001 John Wiley & Sons, Inc. J Biomed Mater Res 59: 378–385, 2002

Key words: ASTM F-75 alloy; solution treatment; carbide; kinetics

INTRODUCTION

The Co–Cr–Mo–C alloy, complying with the ASTM F-75 standard, is used in orthopedic implants.[1,2] The investment cast components of this alloy exhibit a typical microstructure consisting of a Co-based face centered cubic (fcc) matrix showing interdendritic and grain boundary precipitates. It is generally accepted that these precipitates are constituted by a mixture of $M_{23}C_6$ carbides, a σ intermetallic phase and fcc phase.[3] Frequently, a slow cooling during solidification of the alloy or a posterior heat treatment given to the latter promote the occurrence of a lamellar "perlite type" carbide precipitate at the grain boundaries.[4–6] Carbide precipitation represents the main strengthening mechanism in the as-cast conditions; it is also mostly responsible for the low ductility observed under such conditions, which is frequently insufficient to satisfy the aforementioned standard.[2,7,8] A posterior thermal treatment given to the cast alloy constitutes the alternative method most commonly used to enhance ductility; the usual operation consists of a solution treatment carried out at temperatures around 1473 K for periods ranging from 1 to 4 h. It has been shown that the partial dissolution of carbides can improve not only ductility but also other mechanical properties, specifically yield and ultimate tensile strengths.[9,10]

Although the results reported in the literature indicate that an adequate solution treatment improves the mechanical properties of the as-cast alloy, a wide variation still exists in the values of the resultant properties as well as in the variables involved, particularly with regard to the chemical composition of the alloy, its as-cast microstructure, and time and temperature for the heat treatment.[3,9–12] The as-cast microstructural characteristics of the alloy, namely type, size, and fraction of carbides, depend on the solidification condi-

Correspondence to: M. Herrera–Trejo; e-mail: mherrera@saltillo.cinvestav.mx

Contract grant sponsor: CONACyT; contract grant number: 3522-A

tions as well as on the chemical composition. The content of carbide forming elements together with that of carbon influence the chemical composition of the carbide precipitates. Moreover, it has been shown that short treatment times improve the alloy's mechanical properties, however, prolonged treatment times lead to a ductility gain at the expense of other mechanical properties.[10] Regarding the treatment temperature, this is limited by the melting point of the interdendritic carbide precipitates. It is worthwhile to emphasize the remarkable differences existing among the melting temperatures reported in the literature for the interdendritic carbides. In solution heat treatments conducted by Doobs et al.[10] at 1513 K as well as by Taylor et al.[13] at 1523 K, the melting of the interdendritic carbides was not observed. In contrast, Clemow and Daniell[14] detected the melting of this type of carbides at temperatures as low as 1493 K. Furthermore, Kilner et al.[3] determined a melting temperature of 1508 K for the interdendritic carbides by using thermal analysis techniques.

Although the effect of the solution treatment on the mechanical properties of the alloy is strongly related to the carbide features, studies on the characterization of carbides formed during the solution treatment are really scarce in the literature. Clemow and Daniell[14] studied the reactions taking place during the solution treatment as well as the carbide dissolution kinetics. In their work, the carbide dissolution kinetics was relatively elevated at the onset of the thermal treatment and decreased progressively with the progress of the latter. These authors stated that the $M_{23}C_6$ interdendritic carbide present initially in the as-cast condition was transformed into a M_6C carbide during the thermal treatment. The presence of the latter carbide was associated to the slowing down observed in the carbide dissolution kinetics. It was also observed that the formation of the M_6C carbide was promoted by an increase in the thermal treatment temperature. A series of phase diagrams were proposed to explain the results obtained. It is worthy to note that for the computation of such diagrams, the segregation of Mo was considered nonexistent, and that the M_6C carbide was supposed to be a stable phase. However, posterior studies[14,15] reported a significant segregation of Mo, and the presence of the M_6C carbide in the solution-treated alloy claimed by Clemow and Daniell[14] has caused controversy because the $M_{23}C_6$ carbide has been the only carbide found reported in other similar works.[11,13,14] Hence, the phase diagrams proposed by these authors should be reconsidered.

Another study concerning the characterization of the precipitates in an ASTM F-75 alloy is that conducted by Kilner et al.[3] These authors identified a σ intermetallic phase, a $M_{23}C_6$ carbide, and a fcc phase to be the constituents of the interdendritic precipitates in the as-cast conditions. Their results agreed well with those of Koster and Sperner,[16] which proposed the existence of a ternary eutectic composed by the σ phase, $M_{23}C_6$ carbide, and fcc phase. However, the melting temperature of 1508 K determined by Kilner et al.[3] for the interdendritic material differs remarkably from the eutectic precipitation temperature (1608 K) proposed by Koster and Sperner.[16] Such difference was associated to compositional variations in the employed alloys. Furthermore, in solution treated specimens, the $M_{23}C_6$ carbide was the only carbide observed. In a synthetic specimen having a chemical composition similar to that corresponding to the interdendritic material, Kilner et al.[3] found a M_7C_3 carbide, additionally to the ternary eutectic. In an attempt to explain their findings, these authors suggested the occurrence of an early precipitation of the M_7C_3 carbide followed by formation of the ternary eutectic.

In view of the discrepancies evidenced above, a study aiming to elucidate the mechanism of the carbide transformation taking place during the solution treatment of an ASTM F-75 alloy was undertaken. The carbide chemical composition was followed throughout the solution treatment, which was conducted at a temperature close to that corresponding to the carbide melting temperature. The thermal cycle consisted of two stages: (1) rapid heating of the samples up to a temperature at which a transformation was not observed in the carbides, followed by (2) heating up to a preestablished solution treatment temperature. To evidence a possible carbide transformation occurring during the heating stage, three heating rates were used for the second stage of the thermal cycle.

EXPERIMENTAL PROCEDURE

A Co–Cr–Mo–C alloy complying with the ASTM F-75 standard[17] was employed. By using an induction furnace, the alloy was heated under a vacuum and then melted and cast under argon atmosphere at 1873 K in a ceramic mold preheated at 1223 K. The chemical analysis of the resulting alloy is given in Table I, in which the requirements of the standard are also included. The ceramic mold consisted of six cylindrical cavities of diameter 1.5 cm and depth 11 cm, designed in such a way as to allow all cavities to attain the same filling and cooling conditions to minimize any microstructural variations taking place among the solidified bars. To eliminate the solidification chill zone from the bars, these were machined to a final diameter of 0.5 cm. Specimens of length 0.6 cm were sectioned from the machined pieces and then encapsulated inside sealed evacuated quartz tubes to prevent oxidation during following solution treatments.

The solution treatment temperature was determined based on the melting temperature of the inter-

TABLE I
Chemical Composition of the Cast Alloy

	Element (Weight Percent)							
	Cr	Mo	C	Si	Mn	Ni	Fe	Co
ASTM F-75	27–30	5–7	0.35 max	1 max	1 max	1 max	0.75 max	Balance
Alloy	27	6.01	0.22	0.94	0.36	0.73	0.49	Balance

dendritic precipitates, which was estimated by employing conventional thermal analysis to study the solidification process of the alloy. For this, a procedure similar to that described above was used, under the same conditions, except for the fact that the alloy was cast in a ceramic mold consisting of an arrangement of three axially interconnected cylindrical cavities of depth 2.5 cm and diameters 1.2, 1.6, and 2.4 cm. The mold was instrumented with Pt-30%Rh and Pt-6%Rh thermocouples linked to a computer to register the cooling curves. The thermocouples were positioned at the middle point of each cylinder's height. This arrangement allowed obtaining a reliable determination of the interdendritic solidification temperature as a function of cooling rate. The temperature selected for the solution treatment was slightly inferior to that determined for the interdendritic solidification.

Heat treatments were performed in an electric resistance chamber furnace. The thermal cycle consisted of a rapid heating up to a temperature that was high but low enough to preserve the as-cast microstructure, then heating up to a predetermined solution treatment temperature and holding at that temperature for periods of 0, 15, 30, 45, 60, and 120 min. This was followed by quenching in water. The maximum temperature allowable during the rapid heating stage was determined by means of metallographic analysis of specimens, which had been rapidly heated up to several high temperatures and then water quenched. Three different heating rates were used in the subsequent heating stage.

To carry out microstructural observations on the optical and scanning electron microscopes (SEM), the specimens were conventionally prepared by grinding and polishing, followed by electrolytic etching employing a chromic acid solution.[18] An optical microscope coupled to an image analyzer was used for the quantitative determination of the carbide content, which was carried out by measuring 20 fields per sample at 200×. This accounted for a total analyzed area of about 3 mm^2 per specimen. The as-cast and solution treated specimens were then subjected to an electrolytic particle extraction procedure described by Weeton and Signorelli.[4] The particles extracted in this way were analyzed by means of X-ray diffraction.

RESULTS AND DISCUSSION

Interdendritic solidification temperature and thermal cycle

Figure 1 shows the cooling and the cooling rate curves obtained from the thermal analysis of the alloy. The latter curve was obtained from a derivative analysis of the former curve. The cooling rate curve exhibited a peak corresponding to a visible small arrest in the cooling curve, which was associated to the solidification of the interdendritic material. All the solidification temperatures obtained from the studied cylinders were very similar: 1497, 1499, and 1498 K for cylinders with diameters of 12, 16, and 24 mm, respectively. These temperatures agree relatively well with both the temperature of 1508 K determined by Kilner et al.,[3] who used the same technique, and the temperature of 1503 K detected by Clemow and Daniell[14] for solution-treated specimens. The differences observed between the temperatures obtained by both groups of researchers and those determined in the present work may be attributed to compositional variations in the studied alloys. Based on the values determined for the interdendritic solidification temperature, the tempera-

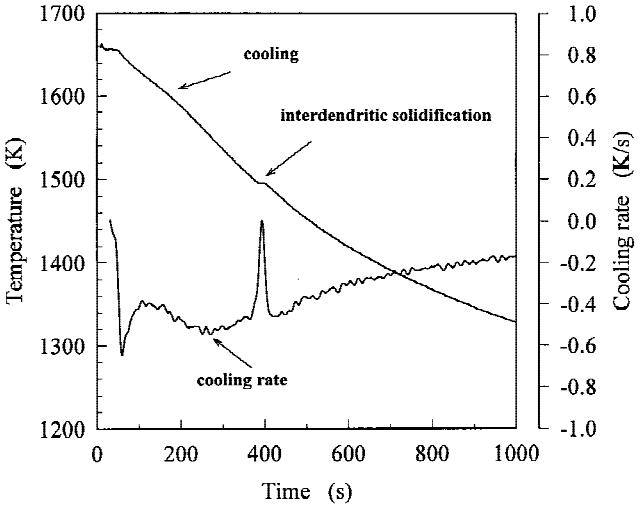

Figure 1. Determination of interdendritic solidification temperature by thermal analysis.

ture selected for the subsequent solution treatments was 1493 K.

In the first heating stage, the metallographic observation of specimens rapidly heated to 1423 K and then water quenched did not indicate the presence of any carbide transformations. In contrast, the presence of cavities was detected along the edges of the carbide particles in specimens rapidly heated to temperatures higher than 1423 K, which were associated to the presence of the σ phase. It is very likely that the cavities were originated from the pull out of the σ phase interdendritic particles during the metallographic preparation of the samples. Therefore, the temperature of 1423 K was chosen as the maximum temperature allowable during the first heating stage, with an average heating rate estimated to be around 345 K/min. For subsequent heating from 1423 to 1493 K, the selected heating rates were 3.3, 10.1, and 16.6 K/min, which gave heating times of 21, 7, and 4 min, respectivley, in this temperature range.

As-cast microstructure

The typical as-cast microstructure observed in this study consisted in Co-rich fcc matrix dendrites and interdendritic and grain boundary precipitates (Fig. 2). The latter precipitates presented film and lamellar morphologies (showing a gray and a dark tone, respectively). The presence of lamellar carbides arises from the thermal conditions used during casting of the alloy, i.e., high mold and metal temperatures.[2] The X-ray diffraction pattern of the electrolytically extracted material (Fig. 3), revealed the presence of a $M_{23}C_6$ carbide and σ phase. It is noteworthy to emphasize that some of the diffraction peaks belonging to both phases are very similar to each other; hence, it is expected that some lines of the diffraction pattern could be the result of the conjunct diffraction of both structures.

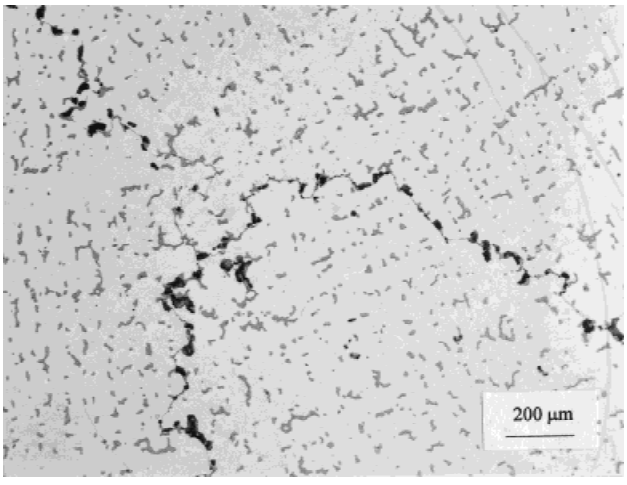

Figure 2. Typical as-cast microstructure.

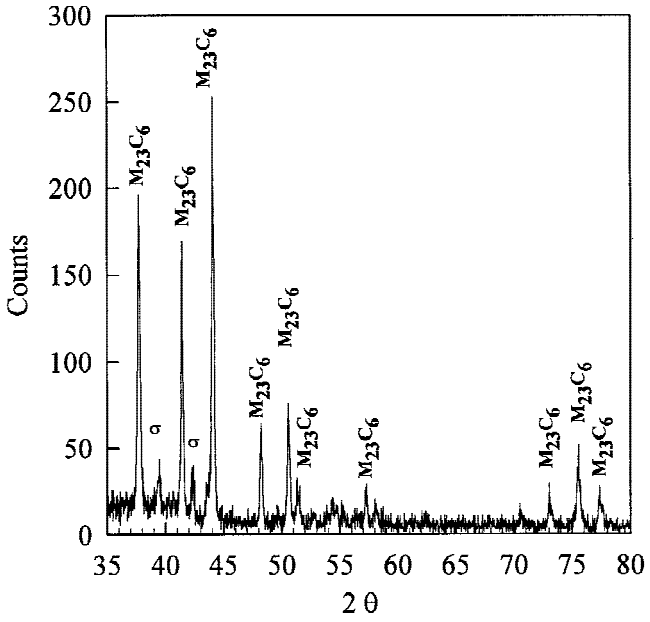

Figure 3. X-ray diffraction pattern of electrolytically extracted precipitates.

Carbide dissolution

The variation of the carbide content with the solution treatment time is shown in Figure 4. The initial

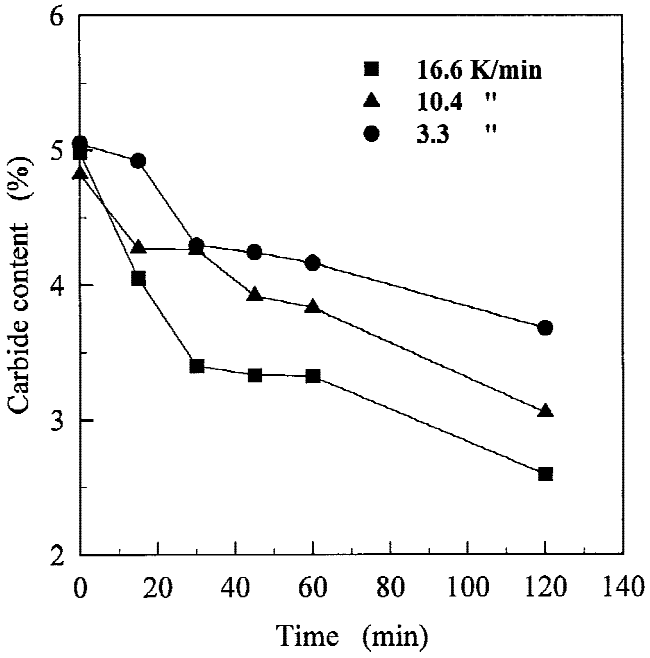

Figure 4. Evolution of carbide content during solution treatment.

values correspond to specimens heated up to 1493 K and then water quenched. As a result of the heating, the carbide content decreased by about 2.5% with respect to that corresponding to the as-cast alloy. This was associated to the dissolution of lamellar precipitates, as expected from the precipitation temperatures previously determined for these precipitates, which was known to be lower than 1493 K.[4–6] Furthermore, it was observed that the kinetics of the carbide dissolution was accelerated by an increase in the heating rate. Figure 5 shows a typical SEM micrograph of the precipitates after 120 min of solution treatment. In all cases, after the heat treatment the precipitates showed a very similar morphology, independently of the heating rate employed, which was characterized by the presence of agglomerates whose size decreased with increasing heating rate.

The X-ray diffraction analysis of the material electrolytically extracted from solution-treated specimens showed that, regardless of the treatment time and heating rate, the constituent of the interdendritic precipitates was a $M_{23}C_6$ carbide. These results agree with those reported by Kilner et al.[3] but differ from those of Clemow and Daniell.[14] The latter authors found the presence of M_6C and $M_{23}C_6$ carbides in solution-treated specimens. To analyze the stability conditions for different carbides, the Thermo-Calc software[20] was used to compute two phase diagrams for the Co–Cr–Mo–C system at the solution treatment temperature employed in the present work (refer to Figs. 6 and 7). These computations required the determination of the chemical composition of the interdendritic precipitates, which represent the phases with maximum content of the carbide forming elements present in the alloy. However, the EDS chemical analysis performed on these precipitates did not produce reliable data, and an effort to employ information given in the literature was unsuccessful due to a remarkable disagreement found among different authors. For instance, Clemow and Daniell[14] reported Mo, C, and Cr contents of 6, 1, and 35%, respectively, in the interdendritic precipitates, while Devine and Wulff[21] determined Mo and Cr contents up to 20 and 35%, respectively. Kilner et al.[3] found a Mo content similar to that

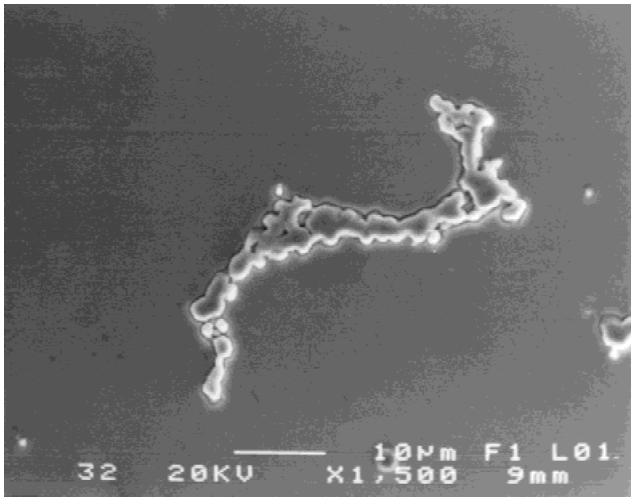

Figure 5. Interdendritic material after 120 min of solution treatment.

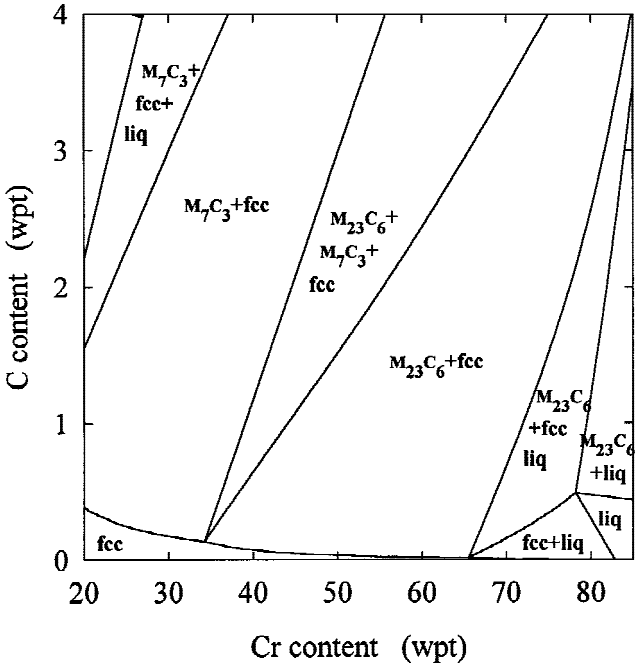

Figure 6. Phase diagram for the system Co–Cr–6% Mo–C at 1493 K.

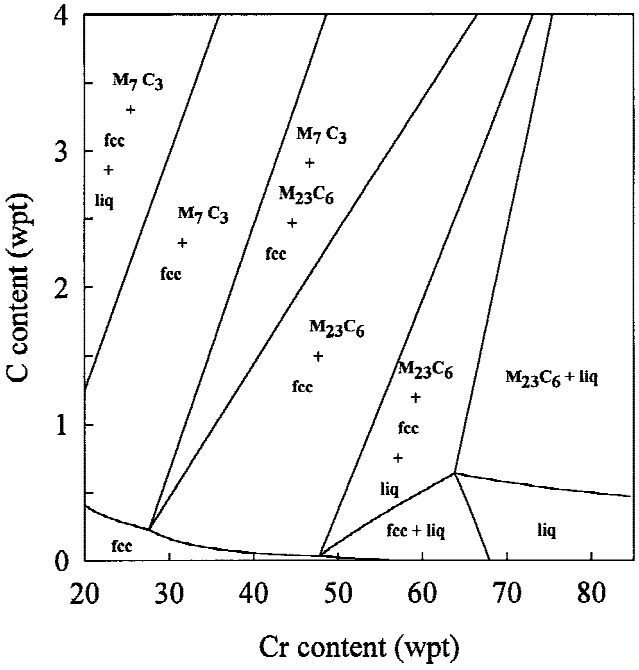

Figure 7. Phase diagram for the system Co–Cr–15% Mo–C at 1493 K.

given by Devine and Wulff,[21] but reported Cr and C contents of 49 and 3.5%, respectively, which are higher than those reported by the authors previously cited. In view of the discrepancies evidenced here, a quantitative description of the stable interdendritic phase, based on published data, was not conceivable. Thus, a qualitative approach was developed to analyze the effect of chemical composition on the stability phase fields. In this way, the phase diagrams of Figures 6 and 7 were computed for 6 and 15% Mo, respectively. The different phases reported in the literature, i.e., $M_{23}C_6$, M_7C_3, M_6C, σ, fcc phase and liquid phase, were considered to be the probable stable phases. By comparing Figures 6 and 7, it is clear that Mo modifies appreciably the relative sizes of the equilibrium phase fields. The absence of a M_6C carbide in both diagrams must be highlighted. This is particularly significant for the diagram of Figure 6, because it is comparable, in terms of chemical composition, to that proposed by Clemow and Daniell,[14] in which the M_6C carbide appears as a stable phase. However, the phase diagram given by the latter authors and that of Figure 6 do agree in that the σ phase is not present, and the $M_{23}C_6$ carbide can be formed. As observed in Figures 6 and 7, the presence of the latter carbide is possible in a wide compositional range. From both figures it can be seen that the $M_{23}C_6$ carbide is found within the $M_{23}C_6$ + fcc field. It is worthy to note that an increase in the Mo content shifts the maximum C content for the latter field toward higher values. Thus, assuming a Mo content higher than 15%, the 3.6% C content proposed by Kilner et al.[3] may be explained.

As previously mentioned, Kilner et al.[3] identified the $M_{23}C_6$ as the only carbide present in a solution-treated alloy. Furthermore, these authors found M_7C_3 and $M_{23}C_6$ carbides in a synthetic material whose chemical composition was claimed to be similar to that corresponding to the interdendritic precipitates. The phase diagram of Figure 7 shows that both carbides can coexist with a fcc phase within a field adjacent to the $M_{23}C_6$ + fcc field. This suggests that the occurrence of the M_7C_3 carbide can be associated to differences in chemical composition between the interdendritic and the synthesized material. For instance, from Figure 7 it is deduced that for a given Cr content the formation of M_7C_3 carbide is promoted by an increase in the C content.

As can be observed in Figure 4, a lower heating rate retarded appreciably the dissolution kinetics of carbides. This effect was attributed to morphological changes induced in the interdendritic precipitates during the heating stage. Specimens heated up to the temperature treatment, using heating rates of 3.3 and 16.6 K/min, and then water quenched, were analyzed on the SEM. Figure 9(a) and 9(b) shows the effect of the heating rate on the morphology of the precipitates. These were observed to consist of a network of agglomerates that got coarser when the heating rate was decreased. Evidently, the employment of lower heating rates caused that the specimens had to be hold at high temperatures during a longer period of time before the treatment temperature was achieved, and this caused coarsening of the agglomerates. The occurrence of this phenomenon reduced the matrix/precipitate interfacial area and, consequently, the dissolution kinetics was affected. The effect of the heating rate can also be explained considering the effect of temperature on the driving force available for the carbide dissolution. Figure 8 depicts a portion of the phase diagram of Figure 5, which was constructed at 1493 K for a Mo content corresponding to that of the studied alloy. In the same figure, an analogous phase diagram constructed at 1423 K was superimposed to the depicted portion of the phase diagram of Figure 5, indicating the chemical composition of the alloy. It can be observed that both diagrams are similar in shape, except for the fact that a decrease in temperature causes a shift toward lower C and Cr contents. From Figure 8 it is inferred that the driving force for the carbide dissolution is increased when a temperature rise displaces the alloy chemical composition toward the fcc phase field. Thus, a rapid increase in the driving force for the carbide dissolution, associated to a high heating rate, promoted the carbide dissolution process.

From the analysis of the kinetic curves shown in Figure 4, it is observed that for all three heating rates studied the carbide dissolution was relatively fast at the onset of the solution treatment, but then it slowed down as the heat treatment progressed. It is known

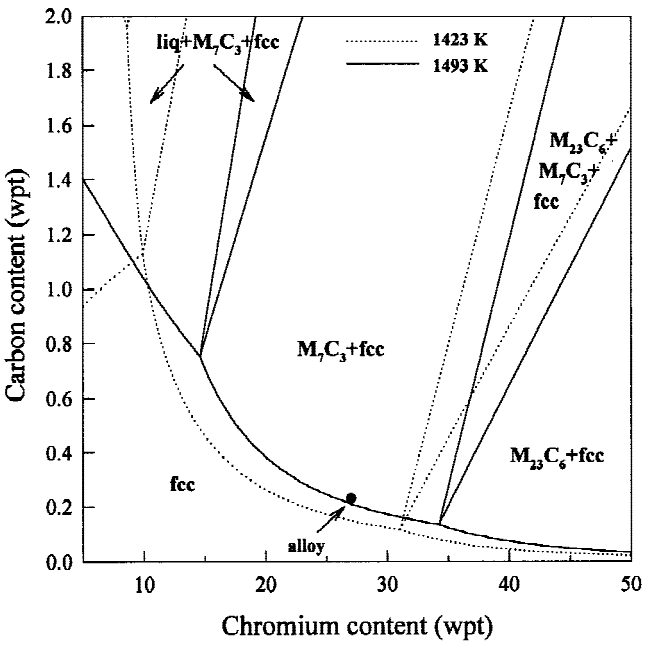

Figure 8. Phase diagram for the system Co–Cr–6% Mo–C at 1423 and 1493 K.

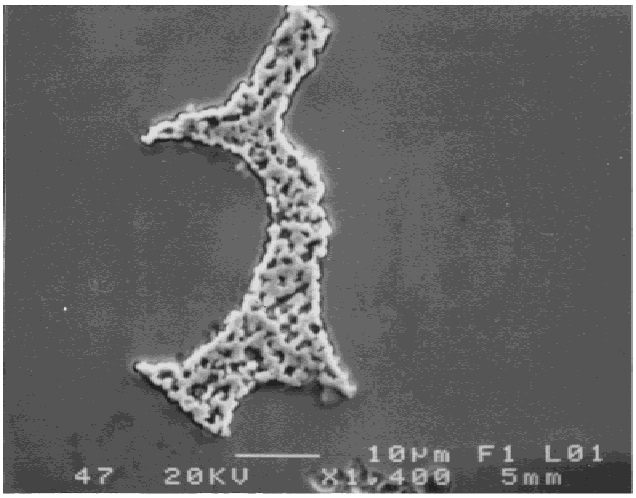

(a)

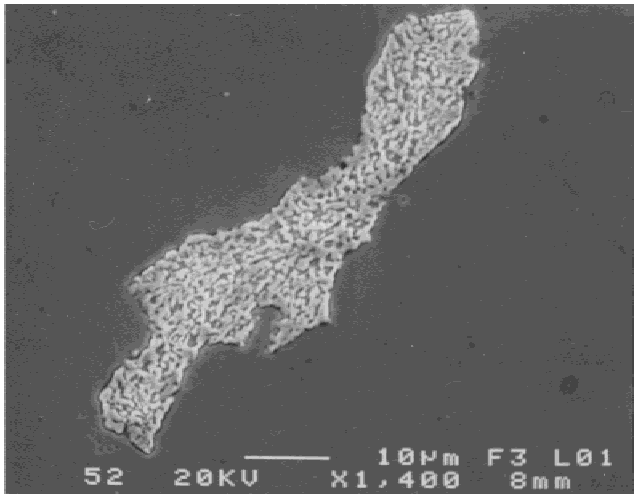

(b)

Figure 9. Interdendritic material after heating stage by using (a) 3.3 and (b) 16.6 K/min as heating rate.

that the driving force for the dissolution process is given by a concentration gradient of a carbide forming element at the matrix/carbide interface.[14] Consequently, the driving force tends to decrease as the carbide dissolution progresses due to the migration of solute atoms out of the carbide. Therefore, the carbide dissolution kinetics is retarded by the redistribution of solute atoms moving away from the carbide/matrix interface. This contrasts with the explanation given by Clemow and Daniell,[14] who attributed the slowness of the carbide dissolution kinetics to the formation of an M_6C carbide.

CONCLUSIONS

The microstructural evolution of an ASTM F-75 alloy during solution heat treatment was studied. The solution treatment was conducted at a temperature close to the carbide melting temperature. The effect of the heating rate on the carbide dissolution was also studied. The obtained results allow for the following conclusions to be drawn.

Thermal analysis during cooling of the studied alloy indicated that the interdendritic precipitates solidified at 1498 K. In the as-cast condition, the precipitates were constituted by an $M_{23}C_6$ carbide, a σ intermetallic phase, and a fcc phase. In specimens subjected to solution treatment for different times, an $M_{23}C_6$ carbide was the only phase found in the precipitates. This indicated that the $M_{23}C_6$ carbide present in the as-cast alloy dissolves directly into the matrix without suffering any previous phase transformation. Computed phase diagrams showed that the $M_{23}C_6$ carbide is stable in a wide compositional range, and the σ phase is not a stable phase at the solution treatment temperature. Contrasting with data reported in the literature, an M_6C carbide was not identified to be a stable phase within the compositional range and temperature of interest. It was also found that the carbide dissolution kinetics was sensitive to the heating rate. This effect was attributed to morphological changes induced in the interdendritic precipitates during the heating stage. A slower heating rate decreased the matrix/precipitate interfacial area due to a coarsening of the agglomerates that constitute the interdendritic precipitates.

M. Herrera wishes to acknowledge the financial support from CONACyT (Mexican National Counsel of Science and Technology), project 3522-A. Thanks are also due to Mr. F. Marquez and T. Caballero for their technical assistance in the microstructural characterization.

References

1. Metals handbook 9th ed, vol. 15. Ohio: ASM; 1988.
2. Asgar K, Peyton FA. Effect of microstructure on the physical properties of Cobalt-base alloys. J Dent Res 1961;40:63–72.
3. Kilner T, Pilliar RM, Weatherly GC. Phase identification and incipient melting in a cast Co–Cr surgical implant alloy. J Biomed Mater Res 1982;16:63–79.
4. Weeton JW, Signorelli RA. Effect of heat treatment upon microstructures, microconstituents, and hardeness of a wrought Cobalt base alloy. Trans ASM 1955;47:815–852.
5. Asgar K, Peyton FA. Effect of casting conditions on some mechanical properties of Cobalt base alloys. J Dent Res 1968;84: 73–86.
6. Salinas AR, Soria MA, López HF. The effect of carbon on the mechanical strength of heat treated cast $Co_{27}Cr_5Mo$ alloys. Warrendale, PA: The Minerals, Metals, and Materials Society; 1996. pp 70–79.

7. Riddihough M. Properties of Cobalt-base investment-cast alloys. Found Trade J 1959;5:421–428.
8. Gómez M, Mancha H, Rodríguez J, Escobedo J, Castro M, Méndez M. Relationship between microstructure and ductility of investment cast ASTM F-75 implant alloy. J Biomed Mater Res 1997;34:157–163.
9. Cohen J, Rose RM. J. Recommended heat treatment and alloy additions for cast Co–Cr surgical implants. J Biomed Mater Res 1978;12:935–937.
10. Dobbs HS, Robertson JLM. Heat Treatment of cast Co–Cr–Mo for orthopaedic implant use. J Biomed Mater Res 1983;18:391–401.
11. Vander Sande JB, Coke JR, Wulff J. Transmision electron microscopy study of the mechanism of strengthening in heat-treated Co–Cr–Mo–C alloys. Metall Mater Trans A 1976;7:389–397.
12. Montero CO, Talavera M, López HF. Effect of alloy preheating on the mechanical properties of as-cast Co–Cr–Mo–C alloys. Metall Mater Trans A 1999;390:611–620.
13. Taylor RNJ. Waterhouse RB. A study of the ageing behaviour of a Cobalt based implant alloy. J Mater Sci 1983;18:3265–3280.
14. Clemow AJT, Daniell BL. Solution treatment of Co–Cr–Mo–C alloy. J Biomed Mater Res 1979;13:265–279.
15. Ramírez EV, Ph.D. Thesis, CINVESTAV Saltillo, México, 2000.
16. Koster VW, Sperner F. Das Dreistoffsystem Kobalt-Chrom-Kohlenstoff. Arch Eisenhuttenwesen 1955;26:555–559.
17. Annual book of ASTM F-75 standards, vol. 3.01. Philadelphia, PA: ASTM; 1989.
18. Metals handbook, vol. 9. Ohio: ASM; 1985.
19. Sullivan CP, Varin JD, Donachie MJ. Cobalt-base superalloys. Ohio: ASM; 1979. p 299–312.
20. Thermocalc Software 1999, Sweden.
21. Devine TM, Wulff J. Cast vs wrought Cobalt-Chromium surgical implant alloys. J Biomed Mater Res 1975;9:151–167.